Title
A Subtype-Specific Function for the Extracellular Domain of Neuroligin 1 in Hippocampal LTP

Journal
Neuron, 76(2)

ISSN
0896-6273

Authors
Shipman, Seth L
Nicoll, Roger A

Publication Date
2012-10-01

DOI
10.1016/j.neuron.2012.07.024

Peer reviewed

Published in final edited form as:
Neuron. 2012 October 18; 76(2): 309–316. doi:10.1016/j.neuron.2012.07.024.

A subtype specific function for the extracellular domain of neuroligin 1 in hippocampal LTP

Seth L. Shipman[1,2] and **Roger A. Nicoll**[1]

[1]Departments of Cellular and Molecular Pharmacology and Physiology, University of California, San Francisco, San Francisco, CA 94158, USA

[2]Neuroscience Graduate Program, University of California, San Francisco, San Francisco, CA 94158, USA

Summary

At neuronal excitatory synapses, two major subtypes of the synaptic adhesion molecule neuroligin are present. These subtypes, neuroligin 1 and neuroligin 3, have roles in synaptogenesis and synaptic maintenance that appear largely overlapping. In this study we combine electrophysiology with molecular deletion and replacement of these proteins to identify similarities and differences between these subtypes. In doing so, we identify a subtype specific role in LTP for neuroligin 1 in young CA1, which persists into adulthood in the dentate gyrus. As neuroligin 3 showed no requirement for LTP, we constructed chimeric proteins of the two excitatory neuroligin subtypes to identify the molecular determinants particular to the unique function of neuroligin 1. Using *in vivo* molecular replacement experiments, we find that these unique functions depend on a region in its extracellular domain containing the B site splice insertion previously shown to determine specificity of neurexin binding.

Introduction

As a class of cells, neurons are unmatched in the variety of cellular processes that they display – from migration, dendrite and axon development, and targeting, to synaptogenesis, spiking, synaptic homeostasis and plasticity. Diversity within the proteome of a neuron is central to this wide range of abilities, with proteins specialized for each individual function. Yet, within the milieu of the proteome are families of related proteins, similar in sequence, but encoded by distinct genes. Determining redundancy and specialization within these families of proteins can be a challenge, as the presence of a shared function among a family of proteins under experimental constraints does not prove the lack of endogenous

Address correspondence to Roger A. Nicoll at, Departments of Cellular and Molecular Pharmacology and Physiology, University of California, San Francisco, 600 16th St., Genentech Hall N272D, San Francisco, CA 94158-2517, (415) 476-2018 telephone, (415) 502-8644 fax, nicoll@cmp.ucsf.edu.

specialization *in vivo* any more than the presence of a unique response to an experimental constraint proves that specialization necessarily exists.

In humans, four major genes encode for a family of proteins termed neuroligins. These single-pass transmembrane proteins are found at postsynaptic sites, where they support the formation and maintenance of synapses through both intracellular, as well as trans-synaptic interactions (Washbourne et al., 2004). A cursory look at the neuroligins reveals high sequence and structural homology and a shared major binding partner in presynaptic neurexin (Ichtchenko et al., 1996). Indeed, this similarity is borne out functionally, as all of the neuroligins promote the formation and maintenance of synapses (Chih et al., 2005; Levinson et al., 2005). However, some notable differences have begun to emerge between the neuroligins, suggesting divergent roles for the individual members of this family.

Most dramatically, differences exist between neuroligin subtypes with regard to expression patterns at excitatory and inhibitory synapses, with neuroligin 1 (NLGN1) and neuroligin 3 (NLGN3) found at excitatory synapses and neuroligin 2 (NLGN2) and NLGN3 found at inhibitory synapses (Budreck and Scheiffele, 2007; Song et al., 1999; Varoqueaux et al., 2004). However, beyond the broad excitatory/inhibitory divide, subtle differences exist specifically between the two major neuroligin subtypes found endogenously at excitatory synapses, NLGN1 and NLGN3. Notably, NLGN1 knockout animals have been shown to have deficits in memory (Blundell et al., 2010; Kim et al., 2008) while NLGN3 has been more strongly linked to autism and impairments in social behavior (Radyushkin et al., 2009). Yet, little has been done to directly compare the physiological roles of these two proteins.

In the present study, we explored for possible functional differences between NLGN1 and NLGN3. Using a variety of *in vivo* and *in vitro* techniques combining both knockdown and molecular replacement of the subtypes, we present novel differences in the physiological roles of these two proteins, most strikingly with respect to plasticity. Specifically, we find that NLGN1 has a clear role in the support of LTP in the hippocampus – in young CA1, but extending into adulthood in the dentate gyrus – a role that is not shared by NLGN3. We provide the first molecular dissection of the physiological differences between these neuroligin subtypes at excitatory synapses and find that the unique functions of NLGN1, both the potency of its synaptogenic phenotype and its role in LTP, depend on the inclusion of the B splice insertion site in its extracellular domain.

Results

NLGN1 is exclusively required for LTP in the adult dentate gyrus

We began this subtype comparison of the excitatory neuroligins by testing for a differential role in the support of adult plasticity. To do so, lentiviruses were produced to express previously validated microRNAs targeting NLGN1 (NLGN1 miR) or NLGN3 (NLGN3 miR). In control experiments using dissociated hippocampal neurons, both constructs were shown to reduce their respective target transcripts by greater than 95% (Figure S1A). These viruses were stereotaxically injected into the hippocampi of four-week-old rats. Ten to twelve days later, acute slices were taken and simultaneous recordings were made from

virally transduced neurons and neighboring control cells in either area CA1 or the dentate gyrus (Figure 1A).

In area CA1, knockdown of NLGN1 had no effect on LTP (Figure 1B). However, a strikingly different phenotype was found in another region of the hippocampus, the dentate gyrus. Knockdown of NLGN1 in dentate granule cells resulted in a complete elimination of LTP (Figure 1C). Knockdown of NLGN3, like that of NLGN1, had no effect on LTP in area CA1 (Figure 1D). Yet unlike NLGN1, knockdown of NLGN3 also had no effect on LTP in the dentate gyrus (Fig. 1E). These results provide the first evidence in support of a requirement for NLGN1 in LTP in the dentate gyrus and establish a unique subtype difference between the two neuroligins.

To further examine the effect of single neuroligin subtype loss on excitatory synapses, we compared the amplitude of excitatory currents in transduced and control cells with each of the miRs in both hippocampal regions. Like LTP, neither AMPAR- nor NMDAR-mediated currents were affected in area CA1 by the NLGN1 miR (Figures 1B′ and S1D). However, in dentate granule cells, NLGN1 knockdown substantially reduced both AMPAR- and NMDAR-mediated currents (Figures 1C′ and S1D). Knockdown of NLGN3 resulted in a phenotype with the same regional dependence – no effect on excitatory currents in area CA1, but reductions in both AMPAR- and NMDAR-mediated currents in the dentate gyrus – although the reductions were of a smaller magnitude than those following knockdown of NLGN1 (Figures 1D′–1E′ and S1C–S1E). Interestingly, while knockdown of either neuroligin resulted in reductions of synaptic strength in the dentate gyrus, only knockdown of NLGN1 affected LTP. Thus, it would appear that there is a segregation of neuroligin function whereby loss of either NLGN1 or NLGN3 leads to reductions in synaptic currents, whereas only loss of NLGN1 prevents the induction of LTP.

Reduction of NMDA currents by NLGN1 knockdown is due to a loss of synapses

Because we observed a reduction in NMDAR-mediated current along with a loss of LTP in cells expressing the NLGN1 miR, we wanted to test whether the LTP deficit was due simply to a reduction in NMDAR signaling at individual synapses. The induction of LTP using a pairing protocol is entirely dependent on Ca^{2+} influx through NMDARs (Nicoll et al., 1988), therefore, a condition that reduces the number of NMDARs per synapse would be expected to display an LTP deficit. However, the induction of LTP using a pairing protocol operates on a synapse-by-synapse basis (Isaac et al., 1996; Matsuzaki et al., 2004). If the knockdown were to result in whole-synapse loss, LTP would still be normal in the remaining synapses. A key issue, therefore, is whether the NMDAR content is altered at individual synapses.

We first addressed this functionally, by collecting mixed spontaneous AMPAR- and NMDAR-mediated currents at −70 mV in the absence of external Mg^{2+}, then washing on APV and collecting the pure AMPAR-mediated currents. The pure AMPAR currents were then subtracted from the mixed currents to give a pure NMDAR-mediated spontaneous current. We performed these experiments using simultaneously recorded NLGN1 miR expressing neurons and neighboring control cells in the dentate gyrus, and collected both evoked and spontaneous currents, using the evoked currents to assess the validity of the technique. The stimulation-evoked, subtracted NMDAR-mediated currents in NLGN1 miR

expressing cells were reduced, as expected, compared to control cells (Figure 2A–2B). Moreover, the magnitude of the reduction was identical to that found when NMDAR currents were measured at +40 mV in the previous experiment (as percent of control, +40 mV, 32.12 ± 5.26; subtracted 23.4 ± 4.92; $p > 0.05$), thus providing validation of the technique. Furthermore, neither the charge transfer of the NMDAR current as a percent of the total charge transfer of the mixed AMPAR/NMDAR current nor the kinetics of the NMDAR current were altered in the evoked response (Figure 2C–2D).

We next analyzed the spontaneous currents in these same cells (Figure 2E) and found a dramatic reduction in the frequency of spontaneous events (Figure 2F), but no change in amplitude of either the mixed current, the pure AMPAR current, or the pure, subtracted NMDAR current (Figure 2G). Like the evoked current, knockdown did not affect the percentage of spontaneous charge transfer accounted for by NMDA current (Figure 2H). We consequently conclude that the reduction in evoked NMDAR currents is functionally due to an all-or-none loss of synapses, while the remaining synapses have normal numbers of NMDARs.

To complement the functional evidence for an all-or-none loss of synapses following neuroligin knockdown, we examined spine density. Following knockdown of NLGN1, we filled transduced dentate granule cells and neighboring control cells with fluorescent dye and imaged their dendrites (Figure 2I). We observed a reduction in spine density in NLGN1 miR expressing cells as compared to control (Figure 2J) of a similar magnitude to the reduction in evoked currents. Spine density in dentate granule cells following the knockdown of NLGN3 was also reduced, confirming that synaptic loss is a general response to neuroligin knockdown (Figure S2A–S2B).

Finally, we performed a coefficient of variation analysis on the paired evoked recordings following neuroligin knockdown. This provides yet another test to discriminate changes in the quantal size, q (the magnitude of response to a quanta of transmitter or, physiologically, the number of receptors per synapse), from changes in quantal content, $N \times P_r$ (the number of release sites multiplied by the probability of release or, restated, the number of functional synapses on a given trial that contribute to the postsynaptic response). Further explanation of this analysis can be found in the Supplemental Experimental Procedures. In the case of NLGN1 knockdown, both the AMPAR- and NMDAR-mediated components of the EPSC yield points that vary along the 45° line, consistent with changes in the number of functional synapses rather than a change in the number of receptors per synapse (Figure 2K). NLGN3 knockdown in the dentate gyrus displayed a similar dependence on quantal content (Figure S2C). Thus, each of these converging lines of evidence points to an all-or-none loss of synapses rather than a within-synapse loss of receptors as the mechanism of the reduction in EPSC magnitude following knockdown of neuroligin. Therefore, the LTP deficit observed upon knockdown of NLGN1 is not due to a simple loss of NMDAR-mediated Ca^{2+} influx, but rather a more intrinsic effect of NLGN1 on the plasticity of a synapse.

Subtype specific synaptic phenotype of NLGN1 expression is dependent on a region in the extracellular domain

Given the clear segregation of function between NLGN1 and NLGN3 with respect to plasticity, we next asked whether discrete sub-domains within the proteins account for this difference. We constructed chimeric proteins of NLGN1, substituting in domains of NLGN3 to identify any regions that confer phenotypic differences. We screened these chimeras by overexpression in hippocampal organotypic slice cultures. Using biolistics to sparsely transfect hippocampal neurons, we co-expressed a NLGN, wild-type or chimera, with three chained microRNAs targeting NLGNs 1–3 to knock down endogenous neuroligins. This knockdown background was previously shown to be crucial for assessing effects of mutated neuroligin constructs (Shipman et al., 2011). As in previous recordings, experimental cell currents are always compared to simultaneously recorded untransfected cells.

Since LTP in the dentate gyrus has been shown to have a postsynaptic mechanism (Colino and Malenka, 1993), one might expect these two neuroligins to differ with respect to the intracellular scaffolding of postsynaptic proteins. Therefore, we first constructed chimeric neuroligins of NLGN1 and NLGN3 with the extracellular domain of NLGN1 and the intracellular domain of NLGN3 and vice-versa to test the relative contribution of these two domains to the phenotypic differences between the neuroligin subtypes. We used the magnitude of enhancement of NMDAR-mediated currents as our readout given that NLGN1 expression more potently enhances the NMDAR-mediated currents than NLGN3 (Figures 3A and 3C). As both neuroligins enhance AMPAR-mediated currents, an enhancement of the AMPAR-mediated current was a requirement for all chimeras included in this analysis. Surprisingly, we found that the phenotypic difference between NLGN1 and NLGN3 segregated with the extracellular rather than the intracellular domains. Specifically, a chimera containing the extracellular domain of NLGN1 with the intracellular domain of NLGN3 (NLGN1-TM-NLGN3) enhanced NMDAR-mediated current to the same degree as full-length NLGN1, while the reverse chimera (NLGN3-TM-NLGN1) exactly mimicked full-length NLGN3 (Figures 3A and 3D). Thus it would appear that the extracellular domains of these neuroligins largely account for the subtype differences in phenotype, while the intracellular domains are exchangeable.

To narrow in on the specific region within the extracellular domain that might account for the unique properties of NLGN1, we constructed six additional chimeras with increasingly more of the NLGN3 extracellular domain and less of NLGN1. We found that chimeras containing at least 326 amino acids from the extreme N-terminus of NLGN1 possessed the typical NLGN1 NMDAR enhancement, whereas chimeras that contained less than 254 amino acids of the NLGN1 N-terminus instead displayed NLGN3 type NMDAR enhancement (Figures 4A and 4E). The difference between NLGN1 and NLGN3 in the region between amino acids 326 and 254 includes an alternatively spliced insertion in NLGN1 previously termed the site B (Ichtchenko et al., 1995) (Figure 3B). Interestingly, inclusion of this B site has been shown to determine the specificity with which NLGN1 binds to specific splice variants of neurexin (Boucard et al., 2005). We tested an additional mutant of NLGN1 with a deletion of eight amino acids in the B site and found that it indeed possessed a NLGN3-type NMDAR enhancement phenotype (Figure S3).

In vivo molecular replacement reveals that the extracellular B site of NLGN1 is required for LTP

We have demonstrated that NLGN1, but not NLGN3, is required for LTP in the adult dentate gyrus, but not adult CA1, and that at least some aspects of the phenotypic difference between expression of NLGN1 and NLGN3 are due to the B site insertion in the extracellular domain of NLGN1. What remains is to determine why NLGN1 is required for LTP in dentate gyrus and not CA1 and whether the B site has ramifications for LTP as well as the baseline synaptogenic phenotype of NLGN1. It has been shown that the dentate gyrus, one of two sites in the brain that incorporates substantial adult born neurons throughout life, remains more plastic into adulthood, perhaps accounting for the susceptibility to loss of a synaptogenic molecule (reviewed: (Deng et al., 2010)). Indeed, previous reports indicate that halting adult neurogenesis reduces the expression of LTP in the dentate gyrus (Massa et al., 2011; Singer et al., 2011). Perhaps then CA1 neurons would be susceptible to a knockdown of NLGN1 at an earlier developmental time point when the initial connections are still forming.

To test this hypothesis we switched to *in utero* electroporations. By introducing the NLGN1 miR construct *in utero* we can check the basal state of synaptic currents and LTP in cells lacking NLGN1 at a very young age (Figure 4A). The additional advantage of the *in utero* electroporations is that we can efficiently co-express a replacement neuroligin construct along with the NLGN1 miR, a manipulation that we could not achieve in the adult due to the limited packaging size of a lentivirus. Consistent with a developmental function for NLGN1 in the support of LTP, we found that LTP was abolished in NLGN1 miR expressing CA1 pyramidal neurons at this young time point (Figure 4B). Moreover, like the adult dentate granule cells, but unlike adult CA1 cells, AMPAR- and NMDAR-mediated currents were reduced by the expression of the NLGN1 miR in young CA1 (Figures 4C and S4A).

Given this susceptibility of LTP in young CA1 pyramidal neurons to knockdown of NLGN1 and the fact that *in utero* electroporations are amenable to molecular replacements, we next tested whether inclusion of the extracellular B site, shown to account for the phenotypic difference in slice culture, would also account for the differential subtype roles in LTP. We co-expressed the NLGN1 miR construct with two different neuroligin chimeras: NLGN1-326-NLGN3, which contains the B site insertion and is phenotypically similar to NLGN1; or NLGN1-254-NLGN3, which lacks the B site insertion and is phenotypically similar to NLGN3. We found that replacement with NLGN1-326-NLGN3 rescued LTP in these young CA1 pyramidal neurons, whereas replacement with NLGN1-254-NLGN3 did not rescue LTP (Figures 4D–E). Each replacement construct rescued the reduction in AMPAR- and NMDAR-mediated synaptic currents that accompanied the knockdown of NLGN1 (Figures 4C and S4B–C) and, again using coefficient of variation analysis, all changes in amplitude found with both the knockdown and replacements were consistent with changes in quantal content rather than alterations in the number of receptors per synapse (Figure S4D). Thus, it would appear that, at these synapses, the presence of the B site insertion in NLGN1 is a defining characteristic of an LTP-competent synapse.

Discussion

This study provides a detailed analysis of the subtype specific role of neuroligin in hippocampal LTP. We find that the presence of NLGN1 containing the alternatively spliced B site insertion is a requirement for the expression of LTP in young CA1 pyramidal cells at a time when initial synaptic connections are being made in abundance. Interestingly, this requirement for NLGN1 persists into adulthood in the dentate gyrus, where the incorporation of adult born neurons requires ongoing synaptic formation and remodeling. The other major neuroligin found at excitatory synapses, NLGN3, which lacks the B site insert, clearly has a function in the formation or maintenance of synapses, but is not required for the support of LTP.

The resistance of adult CA1 pyramidal neurons to knockdown by either neuroligin subtype is interesting. It may be that, in these more mature neurons, the diversity and expression level of other postsynaptic adhesion molecules is quite high, diminishing the response to the loss of any one subtype. A variety of other molecules occupy a similar niche to that of neuroligin including the LRRTM family (Linhoff et al., 2009) and CL1 (Boucard et al., 2012). While our lentiviral-expressed targeting sequences against each neuroligin were quite effective in a mixed hippocampal cell culture, it is possible that knockdown efficiency would differ *in vivo*, which we were unable to assess directly. Finally, stable adult CA1 synapses may be less susceptible to the loss of neuroligin than the newly created or rapidly remodeling synapses found in young CA1 or the dentate gyrus.

In the present study, we found that loss of neuroligin in adulthood led to a reduction in the number of synapses rather than a reduction in the number of AMPA or NMDA receptors per synapse. This is consistent with our previous finding, showing a loss of whole synapses upon knockdown of NLGNs 1–3 in organotypic hippocampal slice culture (Shipman et al., 2011). However, other studies have reported changes in the AMPA/NMDA ratio in the NLGN1 knockout which is at odds with these results (Chubykin et al., 2007; Soler-Llavina et al., 2011). This difference could be the result of differences in methodology, particularly the difference between whole brain germ-line knockouts and sparsely expressed RNAi or the use of paired recording to individually measure changes in AMPAR- and NMDAR-mediated currents versus the use of AMPA/NMDA ratios.

Others have reported impairment of LTP following NLGN1 manipulations. Blundell et al. (2010) reported diminished LTP in a NLGN1 knockout mouse using field potential recordings in CA1, while another group found a loss of LTP in the amygdala following knockdown of NLGN1 (Jung et al., 2010; Kim et al., 2008). In each of these cases however, unlike the present study, the manipulation caused apparent changes in NMDAR functioning and therefore the LTP effects were attributed to the loss of the NMDA-mediated inductive Ca^{2+} influx.

It was quite unforeseen that the major difference in phenotype between overexpressed NLGN1 and NLGN3 would reside in the extracellular domain. This domain is known to mediate both cis- and trans- interactions. Specifically, homo- and heterodimerization have been described as well as binding to the presynaptic neurexins (Arac et al., 2007; Fabrichny

et al., 2007). Based on our chimeric analysis and *in vivo* molecular replacement experiments, it is likely that the alternatively spliced insertion at site B in the extracellular domain of NLGN1 is responsible for its unique functions. Of the neuroligins, only the NLGN1 gene contains the possibility of an insertion at the B splice site, which affects the specificity of neurexin binding. Specifically, NLGN1 containing the B insertion binds preferentially to β-neurexins lacking an insertion at splice site 4 and does not bind the longer form α-neurexins (Boucard et al., 2005). The presence of the B site in neuroligin likely has ramifications for the function of the protein, with a number of previous studies reporting different altered phenotypes of NLGN1 containing the B site that include a more potent synaptogenic phenotype (Boucard et al., 2005), a stronger bias toward excitatory synaptic formation (Chih et al., 2006), and differences in the rate of presynaptic induction (Lee et al., 2010). However, the role of the B site in normal physiological function remains unknown. Here we show, for the first time, a physiological consequence of the B site insertion on synaptic plasticity. We propose that this effect is among the first hard evidence for the emerging model that neuroligin subtypes (along with other postsynaptic adhesion molecules) form a trans-synaptic code via their specific binding to the numerous alternatively spliced variants of neurexin – a code that specifies particular synaptic properties, in this case competence to undergo synaptic plasticity.

Experimental Procedures

Further detail for each section provided in the Supplemental Experimental Procedures.

Experimental Constructs

RNAi targeting sequences have been previously characterized as have RNAi-proof versions of NLGN1 (mouse) and NLGN3 (human) (Chih et al., 2005; Shipman et al., 2011). Variants of these constructs were generated using standard cloning techniques.

Lentiviral production and stereotaxic injection

Lentiviral particles for the viral expression of NLGN1 miR and NLGN3 miR were produced in HEK293T cells and injected bilaterally into the medial hippocampi of 4–5 week old rats.

In utero electroporations

In utero electroporations were performed as previously described with minimal adjustments to achieve hippocampal expression (Walantus et al., 2007).

Hippocampal slice preparation

Acute slices were prepared from adult rats 10–12 days after virus injection or young rats from p11 to p15 after *in utero* electroporation. Hippocampal organotypic slice cultures were prepared from 6–8 day old rats as previously described (Stoppini et al., 1991) and transfected using biolistics.

Anatomy and Imaging

For spine imaging, cells were filled via a patch pipette with Alexa Fluor 568 (Invitrogen) and imaged using confocal microscopy.

Electrophysiological recording

Synaptic currents were elicited by stimulation of either the Schaffer collaterals or perforant path when recording from CA1 cells or dentate granule cells, respectively. AMPAR- and NMDAR-mediated responses were collected in the presence of 100μM picrotoxin and 10μM gabazine to block inhibition. LTP was induced via a pairing protocol of 2 Hz stimulation for 90 seconds at a holding potential of 0 mV.

Supplementary Material

Refer to Web version on PubMed Central for supplementary material.

Acknowledgments

This work was supported by grants from the US NIMH. We wish to thank K. Bjorgan and M. Cerpas for technical assistance and J. Levy for comments on the manuscript. We are additionally grateful for assistance provided by the R. Malenka laboratory in lentiviral production methodology.

References

Arac D, Boucard AA, Ozkan E, Strop P, Newell E, Sudhof TC, Brunger AT. Structures of neuroligin-1 and the neuroligin-1/neurexin-1 beta complex reveal specific protein-protein and protein-Ca2+ interactions. Neuron. 2007; 56:992–1003. [PubMed: 18093522]

Blundell J, Blaiss CA, Etherton MR, Espinosa F, Tabuchi K, Walz C, Bolliger MF, Sudhof TC, Powell CM. Neuroligin-1 deletion results in impaired spatial memory and increased repetitive behavior. J Neurosci. 2010; 30:2115–2129. [PubMed: 20147539]

Boucard AA, Chubykin AA, Comoletti D, Taylor P, Sudhof TC. A splice code for trans-synaptic cell adhesion mediated by binding of neuroligin 1 to alpha- and beta-neurexins. Neuron. 2005; 48:229–236. [PubMed: 16242404]

Boucard AA, Ko J, Sudhof TC. High Affinity Neurexin Binding to Cell Adhesion G-protein-coupled Receptor CIRL1/Latrophilin-1 Produces an Intercellular Adhesion Complex. J Biol Chem. 2012; 287:9399–9413. [PubMed: 22262843]

Budreck EC, Scheiffele P. Neuroligin-3 is a neuronal adhesion protein at GABAergic and glutamatergic synapses. Eur J Neurosci. 2007; 26:1738–1748. [PubMed: 17897391]

Chih B, Engelman H, Scheiffele P. Control of excitatory and inhibitory synapse formation by neuroligins. Science. 2005; 307:1324–1328. [PubMed: 15681343]

Chih B, Gollan L, Scheiffele P. Alternative splicing controls selective trans-synaptic interactions of the neuroligin-neurexin complex. Neuron. 2006; 51:171–178. [PubMed: 16846852]

Chubykin AA, Atasoy D, Etherton MR, Brose N, Kavalali ET, Gibson JR, Sudhof TC. Activity-dependent validation of excitatory versus inhibitory synapses by neuroligin-1 versus neuroligin-2. Neuron. 2007; 54:919–931. [PubMed: 17582332]

Colino A, Malenka RC. Mechanisms underlying induction of long-term potentiation in rat medial and lateral perforant paths in vitro. J Neurophysiol. 1993; 69:1150–1159. [PubMed: 8492154]

Deng W, Aimone JB, Gage FH. New neurons and new memories: how does adult hippocampal neurogenesis affect learning and memory? Nat Rev Neurosci. 2010; 11:339–350. [PubMed: 20354534]

Fabrichny IP, Leone P, Sulzenbacher G, Comoletti D, Miller MT, Taylor P, Bourne Y, Marchot P. Structural analysis of the synaptic protein neuroligin and its beta-neurexin complex: determinants for folding and cell adhesion. Neuron. 2007; 56:979–991. [PubMed: 18093521]

Ichtchenko K, Hata Y, Nguyen T, Ullrich B, Missler M, Moomaw C, Sudhof TC. Neuroligin 1: a splice site-specific ligand for beta-neurexins. Cell. 1995; 81:435–443. [PubMed: 7736595]

Ichtchenko K, Nguyen T, Sudhof TC. Structures, alternative splicing, and neurexin binding of multiple neuroligins. J Biol Chem. 1996; 271:2676–2682. [PubMed: 8576240]

Isaac JT, Hjelmstad GO, Nicoll RA, Malenka RC. Long-term potentiation at single fiber inputs to hippocampal CA1 pyramidal cells. Proc Natl Acad Sci U S A. 1996; 93:8710–8715. [PubMed: 8710936]

Jung SY, Kim J, Kwon OB, Jung JH, An K, Jeong AY, Lee CJ, Choi YB, Bailey CH, Kandel ER, Kim JH. Input-specific synaptic plasticity in the amygdala is regulated by neuroligin-1 via postsynaptic NMDA receptors. Proc Natl Acad Sci U S A. 2010; 107:4710–4715. [PubMed: 20176955]

Kim J, Jung SY, Lee YK, Park S, Choi JS, Lee CJ, Kim HS, Choi YB, Scheiffele P, Bailey CH, et al. Neuroligin-1 is required for normal expression of LTP and associative fear memory in the amygdala of adult animals. Proc Natl Acad Sci U S A. 2008; 105:9087–9092. [PubMed: 18579781]

Lee H, Dean C, Isacoff E. Alternative Splicing of Neuroligin Regulates the Rate of Presynaptic Differentiation. J Neurosci. 2010; 30:11435–11446. [PubMed: 20739565]

Levinson JN, Chery N, Huang K, Wong TP, Gerrow K, Kang R, Prange O, Wang YT, El-Husseini A. Neuroligins mediate excitatory and inhibitory synapse formation: involvement of PSD-95 and neurexin-1beta in neuroligin-induced synaptic specificity. J Biol Chem. 2005; 280:17312–17319. [PubMed: 15723836]

Linhoff MW, Lauren J, Cassidy RM, Dobie FA, Takahashi H, Nygaard HB, Airaksinen MS, Strittmatter SM, Craig AM. An unbiased expression screen for synaptogenic proteins identifies the LRRTM protein family as synaptic organizers. Neuron. 2009; 61:734–749. [PubMed: 19285470]

Massa F, Koehl M, Wiesner T, Grosjean N, Revest JM, Piazza PV, Abrous DN, Oliet SH. Conditional reduction of adult neurogenesis impairs bidirectional hippocampal synaptic plasticity. Proc Natl Acad Sci U S A. 2011; 108:6644–6649. [PubMed: 21464314]

Matsuzaki M, Honkura N, Ellis-Davies GC, Kasai H. Structural basis of long-term potentiation in single dendritic spines. Nature. 2004; 429:761–766. [PubMed: 15190253]

Nicoll RA, Kauer JA, Malenka RC. The current excitement in long-term potentiation. Neuron. 1988; 1:97–103. [PubMed: 2856092]

Radyushkin K, Hammerschmidt K, Boretius S, Varoqueaux F, El-Kordi A, Ronnenberg A, Winter D, Frahm J, Fischer J, Brose N, Ehrenreich H. Neuroligin-3-deficient mice: model of a monogenic heritable form of autism with an olfactory deficit. Genes Brain Behav. 2009; 8:416–425. [PubMed: 19243448]

Shipman SL, Schnell E, Hirai T, Chen BS, Roche KW, Nicoll RA. Functional dependence of neuroligin on a new non-PDZ intracellular domain. Nat Neurosci. 2011; 14:718–726. [PubMed: 21532576]

Singer BH, Gamelli AE, Fuller CL, Temme SJ, Parent JM, Murphy GG. Compensatory network changes in the dentate gyrus restore long-term potentiation following ablation of neurogenesis in young-adult mice. Proc Natl Acad Sci U S A. 2011; 108:5437–5442. [PubMed: 21402918]

Soler-Llavina GJ, Fuccillo MV, Ko J, Sudhof TC, Malenka RC. The neurexin ligands, neuroligins and leucine-rich repeat transmembrane proteins, perform convergent and divergent synaptic functions in vivo. Proc Natl Acad Sci U S A. 2011; 108:16502–16509. [PubMed: 21953696]

Song JY, Ichtchenko K, Sudhof TC, Brose N. Neuroligin 1 is a postsynaptic cell-adhesion molecule of excitatory synapses. Proc Natl Acad Sci U S A. 1999; 96:1100–1105. [PubMed: 9927700]

Stoppini L, Buchs PA, Muller D. A simple method for organotypic cultures of nervous tissue. J Neurosci Methods. 1991; 37:173–182. [PubMed: 1715499]

Varoqueaux F, Jamain S, Brose N. Neuroligin 2 is exclusively localized to inhibitory synapses. Eur J Cell Biol. 2004; 83:449–456. [PubMed: 15540461]

Walantus W, Elias L, Kriegstein A. In utero intraventricular injection and electroporation of E16 rat embryos. J Vis Exp. 2007; 236

Washbourne P, Dityatev A, Scheiffele P, Biederer T, Weiner JA, Christopherson KS, El-Husseini A. Cell adhesion molecules in synapse formation. J Neurosci. 2004; 24:9244–9249. [PubMed: 15496659]

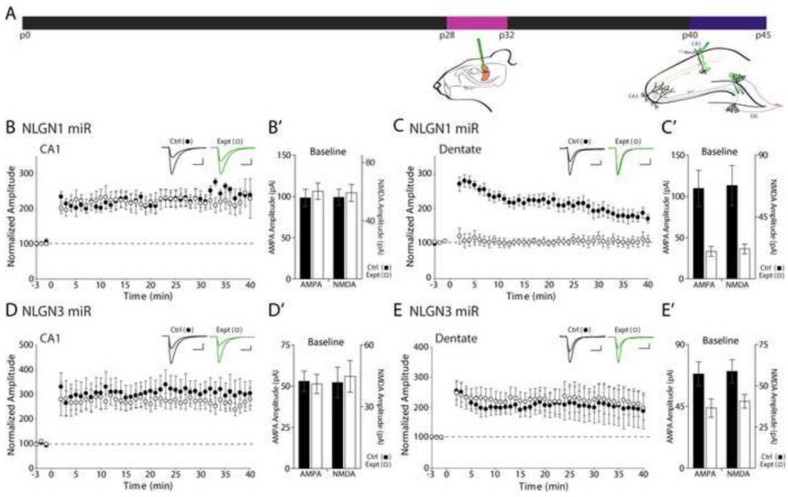

Figure 1.

Role of neuroligin in the expression of adult hippocampal LTP. **(A)** Schematic illustrating the timeline of the lentiviral injections and paired recordings. **(B)** Knockdown of NLGN1 does not affect LTP in area CA1 (n = 6 ctrl, 6 expt), but does eliminate LTP in the dentate gyrus (n = 9 ctrl, 8 expt). For all LTP graphs, control cells are shown as filled circles and experimental cells are shown as open circles. Traces show representative currents from control (in black) and experimental cells (in green) before and after LTP induction (scale bar: 50 pA/20 ms). (**B′)** Bar graph (means ±SEM) shows no effect of the NLGN1miR on baseline AMPAR- ($p > 0.05$, n = 12) or NMDAR-mediated ($p > 0.05$, n = 10) currents based on paired recordings in CA1. **(C and C′)** Knockdown of NLGN1 does eliminate LTP in the dentate gyrus (n = 9 ctrl, 8 expt) and also results in baseline reductions of both AMPAR- ($p < 0.001$, n = 16) and NMDAR-mediated ($p < 0.005$, n = 9) currents. Graphs and sample traces are analogous to those in B. (**D and D′**) Knockdown of NLGN3 does not affect LTP (n = 9 ctrl, 7 expt) or baseline currents (AMPAR: $p > 0.05$, n = 13; NMDAR: $p > 0.05$, n = 10) in CA1 and also (**E and E′**) does not affect LTP in dentate gyrus (n = 7 ctrl, 7 expt), but does reduce both AMPAR- ($p < 0.001$, n = 15) and NMDAR-mediated ($p < 0.01$, n = 12) currents. As in B, traces show representative currents from control (in black) and experimental cells (in green) before and after LTP induction (scale bar: 100 pA/20 ms). Paired recordings used to generate baseline bar graphs shown in Figure S1.

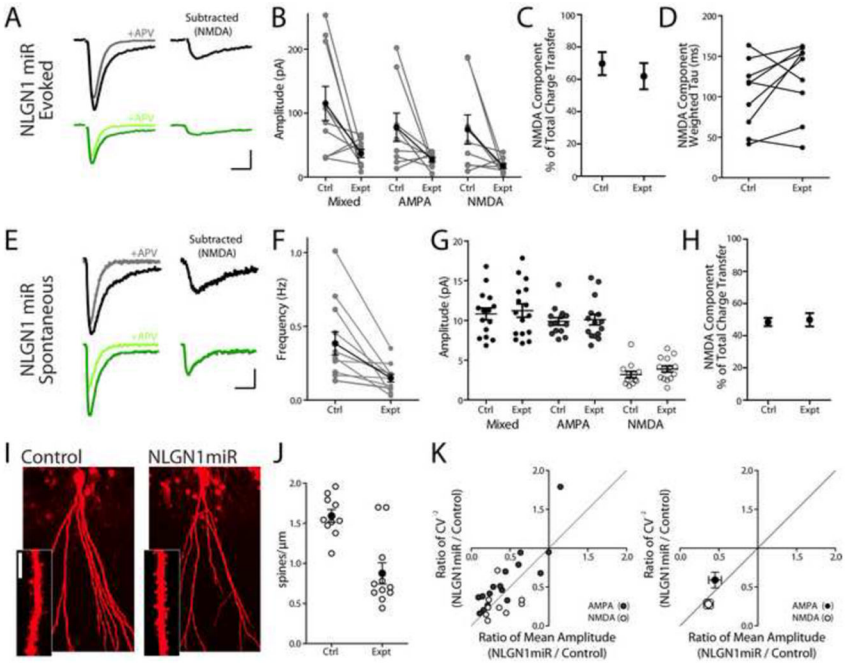

Figure 2.

Knockdown of NLGN1 results in a reduction in the number of functional synapses in the dentate gyrus. **(A)** Representative evoked currents recorded during this experiment showing, to the left, mixed AMPAR/NMDAR-mediated currents from a control cell (in black) and a cell expressing the NLGN1miR (in dark green) and pure AMPAR-mediated currents after the addition of APV from the same control cell (in grey) and experimental cell (in light green). To the right is shown the pure NMDAR-mediated, subtracted current from the control (in black) and experimental cells (in dark green). Scale bar: 20 pA/20 ms. **(B)** Knockdown of NLGN1 results in reductions in the evoked amplitude of the mixed current ($p < 0.05$, $n = 10$), a trend toward reductions in the pure AMPAR-mediated current ($p = 0.0547$, $n = 9$), and reductions in the subtracted, NMDAR-mediated current ($p < 0.05$, $n = 9$). Grey points with connecting lines indicate individual paired recordings, while black points indicate means ±SEM. **(C)** Evoked NMDAR-mediated charge transfer as a percentage of the total mixed charge transfer of the evoked response shown as mean ±SEM ($p > 0.05$, $n = 10$). **(D)** Weighted decay tau of the NMDAR-mediated component of the evoked current. Points with connecting lines indicate individual pairs ($p > 0.05$, $n = 9$). **(E)** Representative currents shown exactly as in A, except for spontaneous rather than evoked currents (scale bar: 4 pA/20 ms). **(F)** Knockdown of NLGN1 results in a reduced frequency of spontaneous currents ($p < 0.001$, $N = 12$). Grey points with connecting lines indicate individual paired recordings, while black points indicate means ±SEM. **(G)** Knockdown of NLGN1 does not alter the amplitude of spontaneous mixed currents ($p > 0.05$, $n = 15$ ctrl, 16 expt), pure AMPAR-mediated currents ($p > 0.05$, $n = 14$ ctrl, 15 expt), or subtracted, NMDAR-mediated currents ($p > 0.05$, $n = 12$ ctrl, 14 expt). Points indicate individual recordings, while bars indicate means ±SEM. **(H)** Spontaneous NMDAR-mediated charge transfer as a percentage of the total mixed charge transfer of the spontaneous response shown as mean ±SEM ($p > 0.05$, $n = 9$). **(I)** Representative dye-filled dentate granule cells to use for spine density analysis. Scale bar: 5 µm. **(J)** Knockdown of NLGN1 results in a reduction in the spine density as compared to control ($p < 0.005$, $n = 10$ ctrl, 11 expt). **(K)** Coefficient of variation analysis for paired recordings of NLGN1miR expressing cells and control cells in the dentate gyrus, consistent with changes in quantal content. Left graph plots individual pairs (AMPA $n = 16$; NMDA $n = 9$), right graph plots mean ±SEM. In each case, AMPAR responses are indicated by filled circles and NMDAR responses are indicated by open circles.

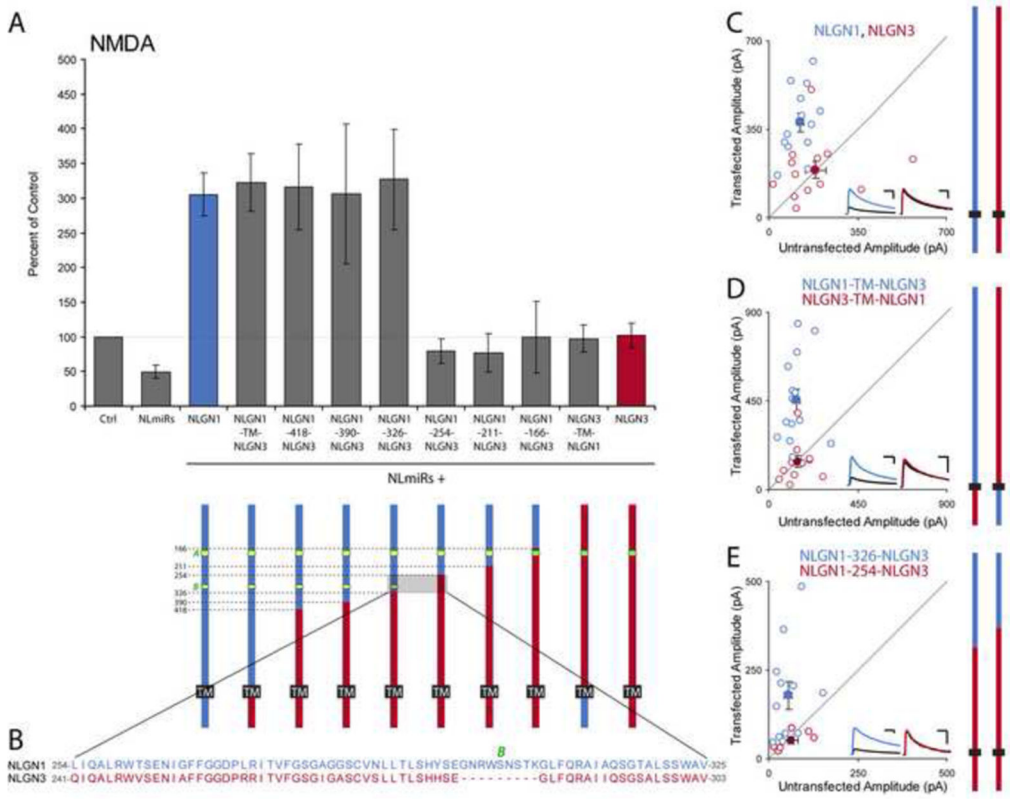

Figure 3.

Differences in expression phenotype between NLGN1 and NLGN3 are due to a difference in the extracellular domain. **(A)** Bar graph showing the effect of overexpression of NLGN1, NLGN3 or chimeras of the neuroligins on the background of a neuroligin knockdown (NLmiRs). Bar showing the NLmiR knockdown phenotype alone was previously published (Shipman et al., 2011) and is repeated here for clarity. Increases in NMDAR-mediated currents as compared to control can be seen on this background with the expression of either full-length NLGN1 ($p < 0.001$, $n = 13$) or a chimera that contains the extracellular domain of NLGN1 and the intracellular domain of NLGN3 (NLGN1-TM-NLGN3, $p < 0.001$, $n = 14$). No increase above control is found upon expression of either full-length NLGN3 ($p > 0.05$, $n = 13$) or a chimera containing the extracellular domain of NLGN3 and the intracellular domain of NLGN1 (NLGN3-TM-NLGN1, $p > 0.05$, $n = 12$). Inclusion of at least 326 amino acids from the N-terminus of NLGN1 in the chimera confers an enhancement of NMDAR responses (NLGN1-418-NLGN3, $p < 0.005$, $n = 13$; NLGN1-390-NLGN3, $p < 0.05$, $n = 10$; NLGN1-326-NLGN3, $p < 0.005$, $n = 12$), whereas inclusion of 254 or fewer amino acids from the N-terminus of NLGN1 does not (NLGN1-254-NLGN3, $p > 0.05$, $n = 6$; NLGN1-211-NLGN3, $p > 0.05$, $n = 6$; NLGN1-166-NLGN3, $p > 0.05$, $n = 10$). Schematic below represents the gross domain structure of the neuroligins, with a short intracellular domain and long extracellular domain (TM: transmembrane). Blue is used to denote NLGN1, while red marks NLGN3. Two alternatively spliced sites (A, present in both NLGN1 and NLGN3, and B, present only in NLGN1) are marked in green. Amino acid numbers in the chimeras and to the left in the schematic are referenced to NLGN1 and indicate the first amino acid in the chimera that is unique to NLGN3. (**B**) Sequence comparison between NLGN1 and NLGN3 in the region of interest that differs between chimeras NLGN1-326-NLGN3 and NLGN1-254-NLGN3 showing the B site insert in NLGN1. **(C)** Direct comparison of the full-length NLGN1 and NLGN3 on the knockdown background showing a clear difference in enhancement of NMDAR-mediated evoked currents ($p < 0.005$, $n = 13$ NLGN1, 13 NLGN3). For all scatter plots, open circles represent individual paired recordings, while filled circles represent means ±SEM (NLGN1 in blue, NLGN3 in red). Traces show representative currents for each condition, with NLGN1 in blue and NLGN3 in red, each with a

simultaneously recorded control cell (in black) (scale bar: 50 pA/100 ms). **(D)** Direct comparison of the two chimeras of neuroligin expressed on the knockdown background showing the same difference as in C for the NLGN1 extracellular domain-containing chimera (NLGN1-TM-NLGN3) as compared to the NLGN3 extracellular domain-containing chimera (NLGN3-TM-NLGN1) ($p < 0.001$, n = 14 NLGN1-TM-NLGN3, 12 NLGN3-TM-NLGN1). Blue marks NLGN1-TM-NLGN3 and red marks NLGN3-TM-NLGN1. (**E**) Direct comparison of chimeras NLGN1-326-NLGN3 and NLGN1-254-NLGN3 again illustrating the differential enhancement of the NMDAR-mediated evoked currents ($p < 0.05$, n = 12 NLGN1-326-NLGN3, 6 NLGN1-254-NLGN3). Blue marks NLGN1-326-NLGN3 and red marks NLGN3-254-NLGN1.

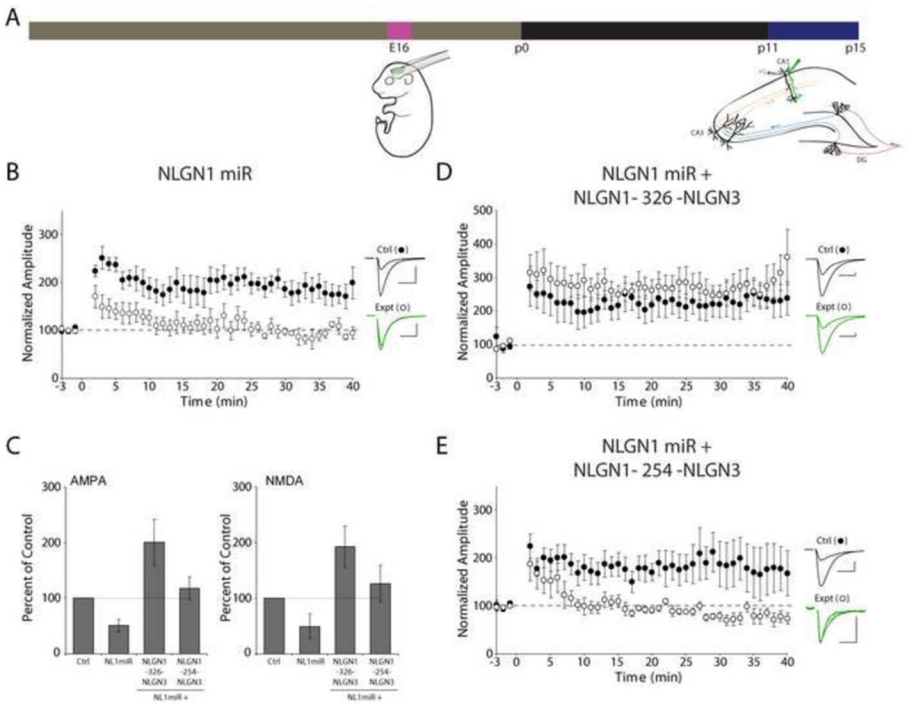

Figure 4.

Role of NLGN1 and the B site insertion in its extracellular domain in young hippocampal LTP. (**A**) Schematic illustrating the timeline of electroporations and paired recordings. (**B**) Knockdown of NLGN1 eliminates LTP in young CA1 (n = 9 ctrl, 7 expt). For all LTP graphs, control cells are shown as filled circles and experimental cells are shown as open circles. Traces to the right show representative currents from control (in black) and experimental cells (in green) before and after LTP induction (scale bar: 40 pA/20 ms). (**C**) Bar graph showing the effects of *in vivo* knockdown of NLGN1 and molecular replacement of NLGN1 with NLGN1-3 chimeras at a young time point. Expression of the NLGN1miR reduces both AMPAR- and NMDAR-mediated EPSCs (AMPA, $p < 0.05$, n = 15; NMDA, $p < 0.05$, n = 8). Co-expression of the NLGN1miR and either neuroligin chimera rescues these reductions (NLGN1-326-NLGN3: AMPA, $p < 0.005$, n = 12; NMDA, $p < 0.005$, n = 12; NLGN1-254-NLGN3: AMPA, $p < 0.005$, n = 13; NMDA, $p < 0.005$, n = 10 versus NLGN1miR alone). Bars indicate means ±SEM, normalized to control. (**D**) Knockdown of NLGN1 plus replacement by NLGN1-326-NLGN3 rescues the LTP deficit found with the knockdown alone (n = 6 ctrl, 6 expt). (**E**) Knockdown of NLGN1 plus replacement by NLGN1-254-NLGN3 fails to rescue LTP (n = 10 ctrl, 7 expt).